An innovative harmonic radar prototype for miniaturized lightweight passive tags tracking

An innovative harmonic radar prototype for miniaturized lightweight passive tags tracking

Stefano Bottigliero*, Daniele Milanesio*, Maurice Saccani*, Riccardo Maggiora*,
Alessandro Viscardi† and Marco Matteo Gallesi†
*Department of Electronics and Telecommunications (DET)
Politecnico di Torino, Torino, Italy
Email: daniele.milanesio@polito.it
†Dipartimento di Scienze Agrarie, Forestali e Alimentari (DISAFA)
Universita' degli Studi di Torino, Torino, Italy

***Abstract*—Harmonic radars can be generally used to track very small (1.5 cm) and lightweight (15 mg) passive tags; as an example, they have been adopted to track various insects for almost 30 years now. In most of the cases, their usage was motivated by the entomological interest in better knowing the habits of the observed insect; in fewer applications, like ours, prevailed the need of protecting the environment from invasive species. However, despite the purpose of the research involving entomological radars, not a lot of engineering resources have been invested during the last decades with the aim of improving what was basically considered a mere tool in the hands of entomologists. The goal of this paper is to show how modern radar techniques, the progresses in the available hardware and a three years long design effort helped us to build and test an harmonic radar system with considerably improved performances. The prototype herein described is able to detect the flight of tagged insects in real time, up to 500 meters with a quite large field of view in elevation, and can be therefore adopted also in harsh environments.**

I. Introduction

Harmonic radars for insect tracking have been used in many applications in the past. Before describing their evolution over time, we would like to outline here their principle of work. A harmonic radar is a system that illuminates a region of space with radiofrequency waves and receives the harmonics of the transmitted frequencies generated by any non-linear device present in the region. The strongest received harmonic is the second one. The received signal can then be processed to find the exact locations (range and direction) of the points causing the generation of these harmonics. The harmonic radar technique is necessary to be able to detect the targets and to suppress all the possible clutter, i.e. the unwanted environmental reflections. Entomological radars exploit these characteristics by means of installing a small lightweight passive transponder, constituted by a wire and a diode, on the insects to be tracked.

Portable systems like *Recco* (for instance the ones described in [1], [2], [3] and [4]) provide rather inaccurate range data, they are limited in distance (few meters) and they can monitor only slow moving targets; they are mainly adopted as supporting tools for capture-mark-recapture operations in specific areas and, hence, their usage is quite limited. Few works on low power and high distances radars have been released ([5]), where advanced transmission techniques such as the Binary Phase-Shift Keying (BPSK) modulation allowed to increase the range distance and reduce the input power with respect to the previously mentioned references. To the best of our knowledge, the only paper documenting a detection above 500 m still is [6], described in detail in [7] and adopted as reference also by [8]; however, that radar can only be operated on flat terrain and can only detect insects flying at very low altitude. To summarize, despite the quite long period of time, the pioneering work described in [6] remains the most adopted harmonic entomological radar so far. We refer the interested reader to [9], [10] and [11] (and included references) for an overview of the most recent applications of radars concerning entomological studies.

With respect to [6], the prototype herein presented is a solid step forward in the field of harmonic radars, being able not only to reach almost 500 m of range, but having improved detection capabilities no longer limited to flat terrain or low altitude. The main application of this prototype has been the tracking of captured specimen of *Vespa velutina*, also known as the yellow-legged hornet, to their nest destined to be destroyed. *Vespa velutina* is a predatory wasp originally from the Southeast Asia ([12]) but currently well established in Southern Europe ([13], [14]) and often spotted in Northern Europe as well ([15]). This giant wasp is not only extremely dangerous for the humans, but it can be considered a lethal threat to honey bees, whose colonies, being a perfect source of proteins for its larvae, are decimated during summer time. Due to its ability to spread over large areas ([16]) and to the damage caused ([17]), the yellow-legged hornet has been recently included in the European invasive alien species list (EU Reg. 1141/2016), that requires Member States to adopt surveillance action plans and control strategies (EU Reg. 1143/2014). This entomological radar is therefore a part of a coordinated effort, together with standard trapping methods, to stop its diffusion in Italy, in particular in the woody and hilly inland of the Ligurian coast, close to the France border.

We would like to stress here that, despite the specific usage done so far, the very same harmonic radar could also be applied to several other insects and small animals (honeybees, caterpillar moths, beetles, butterflies, stinkbugs, etc.), not only to control invasive species, but also to conduct ecological and biological studies, being the only requirement the capability to carry a 15 mg tag. In addition to specific entomological purposes, this system is also suitable for several detection and tracking applications.

II. System architecture

While referring the interested reader to our previous work ([18], [19], [11]) to wholly assess the improvements over time, we would like to herein shortly introduce the overall architecture of our prototype.

Radar systems are generally constituted by a transmitting (TX) module and a receiving (RX) one operating coherently. The TX module works at 9.4 GHz and includes a Local Oscillator (LO), a directional coupler, a Binary Phase (BP) modulator, a Solid State Power Amplifier (SSPA), a Low Pass (LP) filter and a TX antenna. The RX module works at 18.8 GHz and includes a RX antenna, a Low Noise Amplifier (LNA), a High-Pass (HP) filter and a I/Q demodulator. Both systems share a rotary joint and a Field Programmable Gate Array (FPGA) that controls all processes and takes care of the analysis of the received signal.

The missing link between TX and RX systems is the passive lightweight transponder (also herein referred as tag), which doubles the fundamental frequency of the transmitted signal from the radar and retransmits it back to the receiver. The measure of the time delays between the transmitted and received signals allows determining the distances of the transponders; the direction of arrival corresponds to the pointing direction of the mechanically rotating high directivity antennas in the horizontal plane. Figure 1 reports the overall block diagram of the developed entomological radar.

To conclude the summary of this radar prototype, it is important to highlight that the TX frequency, i.e. 9.4 GHz, is a suitable value, being a trade-off between the transponder size and antenna horizontal dimension and free space path loss. The transponder must be small because it must be attached on hornets back without influencing their flying capabilities. At the same time, a high directivity antenna (i.e. big in terms of wavelengths) is required to achieve a high resolution in the horizontal plane. On the other side, free space path loss increases with frequency.

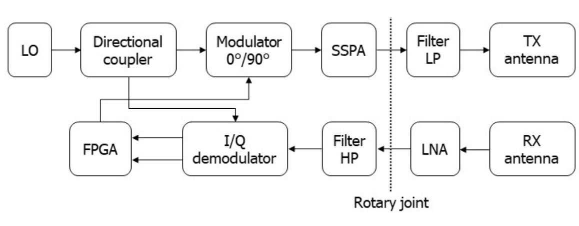

Fig. 1. Harmonic radar block diagram. The rotary joint dashed vertical line divides the rack case containing most of the electronics from the rotating head of the radar, which is made up of the LP filter, the TX and RX antennas and the LNA.

The radar hardware is hosted in a 4U rack case, while the mechanically rotating antennas and the dual channel rotary joint are installed on the top of a telescopic tower. All the system is fed by a commercial portable power generator and a standard laptop is required to immediately visualize the radar output. The Brush Less DC (BLDC) electric motor, responsible of the mechanical rotation, is controlled by the same FPGA processing board through a motor control unit. The programmable rotational speed of the antennas is usually set to 20 rotations per minute, but can be increased if more detections per minute are required. Figure 2 shows the usual radar setup in operative conditions. The total weight of the radar system is approximately 50 kg, while the power consumption is 1 kW.

Fig. 2. Standard radar setup. The TX and RX antennas are visible on top of the system, while the 4U case rack is hanging right below the rotary joint. A telescopic tower helps to operate the radar up to about 6 meters from the soil in order to avoid obstacles, such trees or bushes.

A. The TX module

As anticipated, the TX module of our harmonic radar includes a 9.4 GHz dielectric resonator LO, which is required to achieve an excellent frequency stability, a very low phase noise and very good second harmonic suppression. A Raditek R-DRO-B model has been adopted. Right after the LO, a directional coupler is needed to split the power between the TX modulator and the RX demodulator according to a defined ratio. We adopted the 10 dB directional coupler NARDA 4247B10 that presents a very limited insertion loss.

The core of the TX module is the modulator, which is responsible to perform an On Off Keying (OOK) modulation and a BPSK. To perform these operations we use two Hittite HMC347 two-ways RF switches. The two inputs of the first RF switch are connected on one side to the Raditek RDRO-B-9.41G 9.41 GHz oscillator signal (through the directional coupler) while on the other to a 50 Ω load. The RF switch is driven by a control signal that chooses between the two inputs. The signal is then sent to a Wilkinson power divider, implemented in microstrip technology, designed to split the power equally between the two output branches. The two branches are connected to two delay lines, one $\lambda/4$ longer than the other, to create a 90° phase shift between the two paths. These two lines feed the inputs of the second RF switch. A second control signal, responsible for the BPSK modulation, is used to drive the second RF switch. A phase difference of 90° (instead of the classical 180°) is due to the fact that the transponder doubles both the frequency and the phase of the impinging signal. The two control signals are generated by the FPGA and have a 0V to 2.5V dynamic. In order to fit the RF switches dynamic, that requires the input to be in the range from 0 to -5 volts, they need to be properly conditioned. The complete modulator is realized on a four layers 7 cm by 6 cm board shown in Figure 3. The top layer, where all the RF signals and RF chips resides, is a 35 μm copper layer over a 10 mils RO4350B Roger core. The connections to the underlying RF ground layer are implemented with blind vias. The third layer is the reference ground for the digital signals and it is connected to the RF ground using a single Ω Ohm resistor. To reduce noise coupling, the two planes are not overlapping. The bottom layer hosts all the digital components and related power supply.

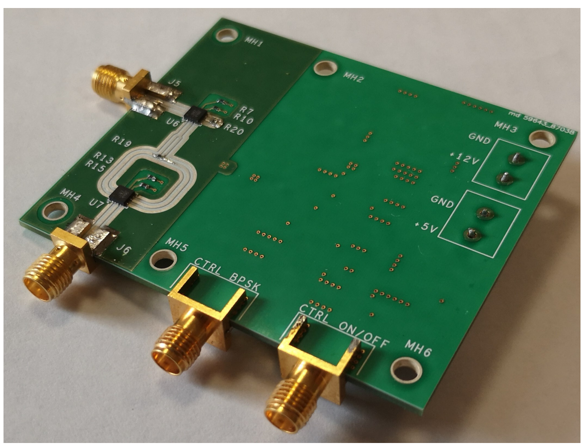

Fig. 3. Top view of the BPSK modulator board.

The modulated signal is amplified to 1 kW by a Gallium Nitride (GaN) SSPA produced by COMTECH PST (BPMC928109-1000). The amplified signal is then filtered and sent to the transmitting antenna through a dual channel rotary joint. A commercial WR90 waveguide filter is required to reduce the unwanted emissions at 18.82 GHz; the LP filter insertion loss is 60 dB at 18.82 GHz.

The 9.4 GHz TX antenna is a 150 cm long slotted WR90 waveguide with 50 radiating elements (horizontal slots, vertical polarization), uniformly tapered along the waveguide direction to reduce side lobes. The TX antenna also mounts two flanges in order to implement a vertical sectoral horn and, therefore, to get a more accurate radiation pattern on the vertical plane. On the horizontal plane the antenna half power beam width (HPBW) is 1.4°, while it is 24° on the vertical plane; the antenna gain is approximately 26.6 dBi.

B. *The transponder (tag)*

The adopted transponder is made up of two metallic pieces connected to a Schottky diode that generates harmonics of the received signal and retransmit it back to the receiving station. Since it has to be attached on the hornet's back, the transponder must be small and lightweight to minimize the effect on the movements and must be installed vertically to be always detected by the radar whatever the hornet position.

Several typologies of transponders were tested throughout the years, from a "loop" configuration to a "W" one ([19]). After an extensive testing, the optimal solution in terms of retransmitted signal was found to be the "J-bended" one ([11]), with a length of 4 mm and 12 mm for the two branches respectively (0.25 diameter wire), and with the diode soldered across the bend. The overall weight of the transponder is 15 mg. Figure 4 shows a tagged insect.

Fig. 4. Tagged hornet hunting in front of a honeybee hive.

To attach the transponder to the hornet's thorax we adopted an orthodontic glue, which polymerizes in few seconds using a polymerization lamp emitting a high-intensity Ultra Violet light. This allows to quickly install the transponder without any sort of anesthesia and to release the specimen within one minute from its capture. Such a procedure is extremely important to maximize the number of insects that fly away once tagged. We also noticed hornets equipped with the transponder preying in front of the hives several days after their capture, clearly indicating that the presence of the tag does not limit their daily routine.

C. *The RX module*

The received signal is collected by the RX antenna mounted on top of the TX one. The 18.8 GHz RX antenna is a 100 cm long slotted WR51 waveguide with 50 radiating elements (horizontal slots, vertical polarization), again uniformly tapered along the waveguide direction to reduce side lobes. Similarly to the TX launcher, also the RX antenna mounts two flanges in order to have a more accurate radiation pattern on the vertical plane. The HPBW on the horizontal and vertical planes are 1.5° and 20° respectively; the antenna gain is approximately 27.3 dBi. It is important to stress that both antennas were entirely designed and manufactured in our laboratory; Figure 5 documents the antenna setup on top of the radar.

Fig. 5. Detailed view of the TX and RX antennas.

Directly connected to the RX antenna and powered by a dedicated battery rotating together with it, there is a high gain LNA manufactured by BZ Technologies. The signal is then passed through the dual channel rotary joint and sent to a BPSK coherent I/Q demodulator, a Hittite HMC570 having the big advantage of hosting internally an active x2 multiplier that can be directly connected to the TX dielectric resonator LO. The demodulated I (In-phase) and Q (Quadrature phase) signals are digitized and delivered to the FPGA processing board.

D. Advanced radar analysis

Due to the low efficiency of passive transponders, high range resolution and high sensitivity, as may be obtained with a transmitted short pulse, are crucial for this application. Unfortunately, the main limitation to achieving high sensitivity with short duration pulses is that a high peak power is required for a large pulse energy. This problem can be solved without losing the short pulse advantages by taking advantage of the so called pulse compression: a transmitted long pulse can be modulated in frequency or phase and the received echoes processed with a proper matched filter. In our case, a long pulse of duration T is divided into N sub-pulses each of width τ. An increase in bandwidth is achieved by changing the phase of each sub-pulse. A common form of phase change is binary phase coding, in which the phase of each sub-pulse is varied within two different values according to some specified criterion. The pulse compression ratio equals the number of sub-pulses $N = T / \tau = BT$, where the bandwidth B is approximately equal to $1/\tau$. Pulse compression filter output will be a compressed pulse of width τ and a peak N times that of the uncompressed pulse. In this case, the optimum filter can be implemented as the correlation between the received echoes with the transmitted sequence. In our prototype radar τ and T are equal to 45 ns and to about 45 μs respectively.

The previously mentioned FPGA board hosts the developed firmware responsible to command the modulator and to correlate the received signals with the transmitted sequence in real time, 1000 times per second. The results of the correlation process are sent through an Ethernet connection to a standard laptop PC for the high level processing and output visualization. On the PC, the data are organized in a bi-dimensional matrix per each transmitted pulse where the I and Q signal levels are stored per each range bin (of about 1 m) and angle of arrival bin (of about $0.1°$).

The core of the high level processing is the Doppler shift estimation implemented by performing a Fast Fourier Transform (FFT) per each range-angle bin along a certain programmable number of pulses usually set equal to 32. This brings the total number of bins to be analyzed equal to 500 (range) x 3000 (angle) x 32 (Doppler) = 48 million bins per each antenna revolution!

The output of the FFT is in the Doppler frequency domain, in which the separation into a certain number of bands offers a very flexible approach to further discriminate against fixed and moving targets. Moreover, if moving clutter (such as that from weather, birds or waiving vegetation) appears with a non-zero mean Doppler shift, an adaptive threshold at the outputs of the FFT may be raised accordingly. After thresholding, a maximum detection in the Doppler frequency domain is performed and the magnitude of the maximum peak is sent to averaging and final plotting on a plan position indicator. The system stores all the transponders positions for further replay and geo-localization. A complete graphical user interface permits to set all the radar parameters and to choose output formats.

III. RESULTS

The results reported in this section refer to an on-field campaign taking place in Arcola (close to La Spezia, Western Liguria) during a two days time frame in September 2018; the aim of this campaign was the localization of a hidden nest of *Vespa velutina* by tracking the tagged hornets flight. Figure 6 reports the typical environment in which this entomological radar is operated, i.e. in woody and hilly area where a large field of view on the vertical plane is mandatory. We also refer the interested reader to [11] for the first validation of the current radar prototype, where a maximum detection distance of about 500 m was verified.

Figure 7 documents all the traces recorded during the Arcola campaign. The radar was first positioned on the right (green cross), in a dominant position with respect to a honeybee hive (white square) in which hornets presence was previously reported. A single insect was tagged and followed during the day, moving the radar in different positions from the right to the left of the map, as documented by the colored crosses.

Even though the radar detections should be analyzed in a statistical way, thus requiring a relevant number of tagged insects to provide preferential directions of flight along which the radar itself should be moved to get closer to the hornets nests, in this specific campaign only a single specimen of *Vespa velutina* was available during the first day. The immediate consequence of having only one tagged insect available was the time required to get at least a few flight paths before moving the radar, which explained the need of more than one day of operations.

During the second day, more hornets were captured also in two other honeybee hives (not shown in the map, but indicated by the arrows), allowing to record more traces and to finally spot the hornets nest, shown with a star on the map. The reader

Fig. 6. One of the radar positions during the Arcola campaign. This is the typical harsh environment in which the radar has to be operated in the Ligurian inland. The top-left zoomed view shows the hornets nest spotted by the entomological radar.

may notice that the nest was in a quite convenient position in order to get food from all the local honeybee hives around it.

The position of the nest was also quite clearly revealed by analyzing the flight speed of the hornets. In fact, when a specimen was flying from the nest to the hunting zone (one of the honeybee hives) the speed was considerably higher than the one registered during the flight back to the nest, due to the weight of the carried prey, i.e. 8 m/s vs. 4 m/s.

To conclude, Figure 6 also reports, in the top-left corner, a zoomed view of the hornets nest that, despite its size (almost half meter in diameter, located at about 25 m from the soil), is basically invisible at bare eye, well hidden in a tall leafy tree.

IV. Conclusions

Insect tracking with the help of harmonic radars is a 30 years long practice, even though performed in quite convenient flat environments. In this paper we describe a new harmonic radar which can be operated also in harsh environment, allowing to track miniaturized lightweight passive tags installed on insects flying in a hilly and woody landscape.

This innovative harmonic radar adopts binary phase modulated transmitted signal at 9.4 GHz to achieve high sensitivity and to be able to maintain good range resolution. Using the results of the correlation between the received demodulated echoes at 18.8 GHz and the transmitted binary code, we can

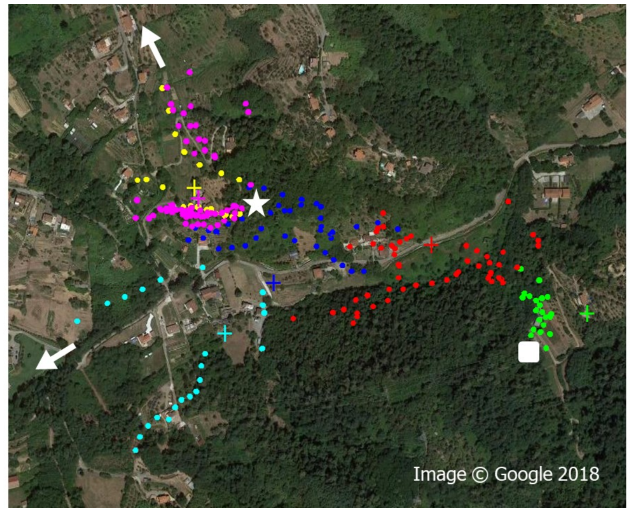

Fig. 7. Georeferenced tracks recorded during the two days long campaign in Arcola, in a 800x675 meters map. The entomological radar was moved in several locations indicated by the crosses, while the square and the arrows reports the position of three honeybee hives. The star refers to the hornets nest.

compute the distance of the transponders. The processing gain from the correlation improves the sensitivity with the number of sub-pulses in the transmitted sequence. An advanced Doppler filtering technique has been also implemented to further suppress the local leakage and the remaining clutter. A further advantage of the system is the possibility to operate it without interruption, day and night, and with any weather condition.

All the parts of this prototype have been designed and manufactured or procured. The final system consists of a 4U rack case, containing most of the hardware, connected to the antennas through a dual channel rotary joint and operated on a trellis; a graphical user interface running on a laptop PC manages all radar outputs and input parameters.

All the hardware and software improvements described in the previous section allowed to effectively adopt this radar for the eradication of *Vespa velutina* in Northern Italy. It is however crucial to stress out that such a powerful tool can be used not only to perform ecological and biological studies on more insects and small animals, but can also be adopted in a broader spectrum of tracking applications.

During 2018 summer, this prototype was daily used to locate Asian hornets nests. Next steps will be focused on improving the usability, flexibility and maneuverability of the radar and, in parallel, the system engineering for the production of a certain number of units.

Acknowledgment

The present work has been funded by the project LIFE14/NAT/IT/001128 STOPVESPA. The authors gratefully acknowledge the valuable support of all the people involved, particularly Dr. G. Dassano for his precious help in the radar assembly, prof. Marco Porporato for his expertise as entomologist and Dr. A. Romano and M. Capello for the on-field assistance.

References

[1] D. Mascanzoni and H. Wallin, "The harmonic radar: a new method of tracing insects in the field," *Ecological Entomology*, vol. 11, no. 4, pp. 387–390, 1986.

[2] R. D. Brazee, E. S. Miller, M. E. Reding, M. G. Klein, B. Nudd, and H. Zhu, "A transponder for harmonic radar tracking of the black vine weevil in behavioral research," *Transactions of the ASAE*, vol. 48, no. 2, pp. 831–838, 2005. [Online]. Available: http://handle.nal.usda.gov/10113/5501

[3] K. T. Hall and M. G. Hadfield, "Application of harmonic radar technology to monitor tree snail dispersal," *Invertebrate Biology*, vol. 128, no. 1, pp. 9–15, 2009.

[4] G. L. Charvat, E. J. Rothwell, and L. C. Kempel, "Harmonic radar tag measurement and characterization," vol. 2, 2003, pp. 696–699.

[5] Z.-M. Tsai, P.-H. Jau, N.-C. Kuo, J.-C. Kao, K.-Y. Lin, F.-R. Chang, E.-C. Yang, and H. Wang, "A high-range-accuracy and high-sensitivity harmonic radar using pulse pseudorandom code for bee searching," *IEEE Transactions on Microwave Theory and Techniques*, vol. 61, no. 1, pp. 666–675, 2013.

[6] J. R. Riley, A. D. Smith, D. R. Reynolds, A. S. Edwards, J. L. Osborne, I. H. Williams, N. L. Carreck, and G. M. Poppy, "Tracking bees with harmonic radar," *Nature*, vol. 379, pp. 29–30, 1996.

[7] J. R. Riley and A. D. Smith, "Design considerations for harmonic radar to investigate the flight of insects at low altitude," *Computers and Electronics in Agriculture*, vol. 35, no. 23, pp. 151–169, 2002.

[8] J. L. Osborne, S. J. Clark, R. J. Morris, I. H. Williams, J. R. Riley, A. D. Smith, D. R. Reynolds, and A. S. Edwards, "A landscape-scale study of bumble bee foraging range and constancy, using harmonic radar," *Journal of Applied Ecology*, vol. 36, no. 4, pp. 519–533, 1999.

[9] J. W. Chapman, V. A. Drake, and D. R. Reynolds, "Recent insights from radar studies of insect flight," *Annual Review of Entomology*, vol. 56, pp. 337–356, 2011.

[10] G. J. Mazzaro, , A. F. Martone, K. I. Ranney, and R. M. Narayanan, "Nonlinear radar for finding rf electronics: system design and recent advancements," *IEEE Transactions on Microwave Theory and Techniques*, vol. 65, no. 5, pp. 1716–1726, 2017.

[11] R. Maggiora, M. Saccani, D. Milanesio, and M. Porporato, "Modern radar techniques help saving beekeeping economic and cultural heritage from vespa velutina threat," *submitted to Scientific Reports*.

[12] M. E. Archer, "Taxonomy, distribution and nesting biology of the vespa bicolor group (hym., vespinae)," *Entomologist's Monthly Magazine*, vol. 130, no. 1560-63, pp. 149–158, 1994.

[13] J. Haxaire, J. Bouguet, and J. P. Tamisier, "Vespa velutina lepeletier, 1836, une redoubtable nouveauté pour la faune de france (hym. vespidae)," vol. 111 (2), 2006, p. 194.

[14] S. Bertolino, S. Lioy, D. Laurino, A. Manino, and M. Porporato, "Spread of the invasive yellow-legged hornet vespa velutina (hymenoptera: Vespidae) in italy," *Applied Entomology and Zoology*, vol. 51, no. 4, pp. 589–597, 2016.

[15] M. J. Keeling, D. N. Franklin, S. Datta, M. A. Brown, and G. E. Budge, "Predicting the spread of the asian hornet (vespa velutina) following its incursion into great britain," *Scientific reports*, vol. 7, no. 6240, 2017.

[16] Q. Rome, F. J. Muller, A. Touret-Alby, E. Darrouzet, A. Perrard, and C. Villemant, "Caste differentiation and seasonal changes in vespa velutina (hym.: Vespidae) colonies in its introduced range," *Journal of Applied Entomology*, vol. 139, no. 10, pp. 771–782, 2015.

[17] J. R. Beggs, E. G. Brockerhoff, J. C. Corley, M. Kenis, M. Masciocchi, F. Muller, Q. Rome, and C. Villemant, "Ecological effects and management of invasive alien vespidae," *BioControl*, vol. 56, no. 4, pp. 505–526, 2011.

[18] D. Milanesio, M. Saccani, R. Maggiora, D. Laurino, and M. Porporato, "Design of an harmonic radar for the tracking of the asian yellow-legged hornet," *Ecology and Evolution*, vol. 6, no. 7, pp. 2170–2178, 2016.

[19] ——, "Recent upgrades of the harmonic radar for the tracking of the asian yellowlegged hornet," *Ecology and Evolution*, vol. 7, no. 13, pp. 4599–4606, 2017.